Synthesis of New Cationic Schiff Base Complexes of Copper(II) and Their Selective Binding with DNA

Tomohide Tanaka, Keiko Tsurutani,† Atsushi Komatsu,† Toyofumi Ito, Kazumi Iida,† Yuki Fujii,*,† Yoshiharu Nakano,† Yoshiharu Usui,† Yutaka Fukuda,†† and Makoto Chikira†††

Graduate School of Science and Engineering, Ibaraki University, 2-1-1, Bunkyo, Mito 310

†Department of Chimistry, Faculty of Science, Ibaraki University, 2-1-1, Bunkyo, Mito 310

††Department of Chemistry, Faculty of Science, Ochanomizu Women's University, 2-1-1, Otuka, Bunkyo-ku, Tokyo 112

†††Department of Applied Chemistry, Chuo University, 1-13-27, Kasuga, Bunkyo-ku, Tokyo 112

(Received September 6, 1996)

A series of cationic salen-type Schiff base complexes of copper(II), the general formula of which is $[Cu\{R_3N^+–CH_2–C_6H_3(O^-)–CH=N–\}_2X]Br_2$ (R: CH_3, C_2H_5, C_3H_7, C_4H_9; X: C_2H_4, C_3H_6, C_6H_{10}, C_6H_4, $C_{10}H_6$), was newly prepared, and the molecular structure of complex **1** ($R=CH_3$, $X=C_2H_4$) was determined by an X-ray crystal structure analysis. The binding mode and binding constants (K_b) of all the complexes with calf thymus DNA were investigated at an ionic strength of $I=0.05$ (NaCl+HEPES buffer, pH=7.2) using induced CD and the UV-vis spectra. Those complexes with aliphatic X group selectively bound to the groove of DNA, and the K_b's were in the range of 10^2—10^3 mol dm^{-3} (site size base pairs $n=7.2$—7.4). However, those with aromatic X group selectivity intercalated to the base pairs, and the K_b's were in the range of 10^4—10^5 mol dm^{-3} ($n=2.8$—4.0). These binding modes were confirmed based on the salt dependence of K_b's. In addition, **1** and **10** ($R=CH_3$, $X=C_6H_4$) were found to exhibit AT-sequence affinity from the induced CD spectra and K_b's for poly(dA-dT)–poly(dA-dT), poly(dG-dC)–poly(dG-dC), and poly(dA-dC)–poly(dT-dG).

The interaction of transition-metal complexes with nucleic acid is a recent active area of research, particularly concerning the development of new biochemical tools and in designing new drugs.[1,2] In these studies it is essential that metal complexes selectively bind with and/or cleave nucleic acid; many metal complexes have been developed for these purposes. Typical examples are Pt(II)-diamine,[3] Ru(II)- and Rh(III)-polypyridine,[4] Cu(I)-phenanthroline,[5] Fe(II)-EDTA,[6] Mn(III)-porphyrin,[7] and Zn(II)-polyamine[8] complexes.

For metal complexes containing a salen-type Schiff base,[9] an AT-site selective DNA scission has been reported;[9a] however, little is known concerning the interaction mechanism with DNA. Recently, we found that cationic salen-type Schiff base complexes of copper(II) bind with DNA with a high mode selectivity (groove binding or intercalation).[10] In this paper, we first report on the synthesis and structure of a series of cationic Schiff base complexes of copper(II) (Chart 1). Since these complexes were thermodynamically so stable, the binding constants (K_b) and binding mode with calf thymus DNA were investigated in detail using UV-vis and induced CD spectra to confirm the mode selectivity. Further, in order to obtain information concerning site or sequence selectivity, we investigated the induced CD spectra and the binding constants of typical complexes, **1** and **10**, for poly(dA-dT)–poly(dA-dT) (AT-DNA), poly(dG-dC)–poly(dG-dC) (GC-DNA), and poly(dA-dC)–poly(dT-dG) (ACTG-DNA).

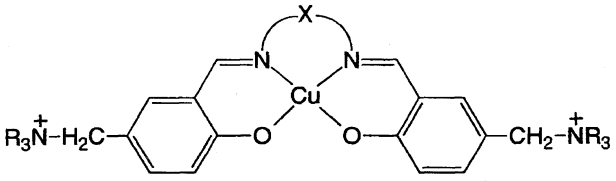

X=$(CH_2)_2$: R=Me(1), Et(2), *n*-Pr(3), *n*-Bu(4)
R=Me and 3,3'-*t*-Bu(5)
X=$\{C(CH_3)_2\}_2$: R=Me(6); X=$(CH_2)_3$: R=Me(7)
X=(*R*,*R*)-C_6H_{10}: R=Me(8); X=(*S*,*S*)-C_6H_{10}: R=Me(9)
X=C_6H_4: R=Me(10), Et(11), *n*-Pr(12), *n*-Bu(13)
X=$C_{10}H_6$: R=Me(14)

Chart 1. Structure and number of complexes.

Experimental

Preparation of Complexes. Since the preparation of all the complexes (**1**—**14**) is very similar to each other, a typical method is described. The elemental analysis data and yield are summarized in Table 1.

An aqueous solution (45 cm^3) of copper(II) acetate dihydrate (2.1×10^{-3} mol) was added to an aqueous solution (20—50 cm^3) of 5-(trialkylammoniomethyl)salicylaldehyde chloride (4.4×10^{-3} mol). To this green solution, a diamine (2.2×10^{-3} mol), which was diluted with a small amount of water, was added, and the pH of the solution was adjusted to about 7.4 with an aqueous NaOH solution. After the solution was stirred for one week at room temperature, the solution pH was again adjusted to 7.4 with an aqueous

Table 1. Elemental Analysis Data, Yield, Color, and Purification Method of the Complexes

Complex	R	X	Elemental analysis/%[a]					Yield	Color	Purification
	Formula		C	H	N	Cu	Br	%		
1	CH_3	$-(CH_2)_2-$	39.93	6.20	7.67	8.56	22.2	80	Purple	Water
	$C_{24}H_{34}N_4O_2Br_2Cu\cdot 5H_2O$		(39.82)	(6.13)	(7.74)	(8.78)	(22.07)			
2	C_2H_5	$-(CH_2)_2-$	47.51	6.73	7.42	8.26	21.4	62	Purple	Water
	$C_{30}H_{46}N_4O_2Br_2Cu\cdot 2H_2O$		(47.78)	(6.68)	(7.42)	(8.43)	(21.19)			
3	*n*-C_3H_7	$-(CH_2)_2-$	49.36	7.40	6.26	7.04	18.4	81	Purple	Methanol
	$C_{36}H_{58}N_4O_2Br_2Cu\cdot 4H_2O$		(49.46)	(7.61)	(6.41)	(7.27)	(18.24)			
4	*n*-C_4H_9	$-(CH_2)_2-$	53.17	8.05	5.96	6.59	16.8	56	Purple	Methanol
	$C_{42}H_{70}N_4O_2Br_2Cu\cdot 3.5H_2O$		(53.13)	(8.17)	(5.90)	(6.69)	(16.83)			
5[b]	CH_3	$-(CH_2)_2-$	50.36	7.97	7.34	8.16	9.0[e]	66	Purple	Methanol
	$C_{32}H_{50}N_4O_2Cl_2Cu\cdot 6H_2O$		(50.22)	(8.17)	(7.32)	(8.30)	(9.26)[e]			
6	CH_3	$-(C(CH_3)_2)_2-$	40.88	6.01	6.79	7.69	24.1	20	Purple	Water–acetone
	$C_{28}H_{42}N_4O_2Br_2Cu\cdot 4H_2O\cdot 0.5KBr$		(40.93)	(6.13)	(6.82)	(7.73)	(24.31)			
7	CH_3	$-(CH_2)_3-$	44.77	5.63	8.34	9.16	24.4	74	Green	Water–acetone
	$C_{25}H_{36}N_4O_2Br_2Cu\cdot 1.5H_2O$		(44.49)	(5.82)	(8.30)	(9.41)	(24.66)			
8	CH_3	$-C_6H_{10}-$[d]	43.48	6.22	7.41	8.08	21.0	75	Purple	Water
	$C_{28}H_{40}N_4O_2Br_2Cu\cdot 5H_2O$		(43.22)	(6.48)	(7.20)	(8.17)	(21.03)			
9	CH_3	$-C_6H_{10}-$[e]	43.06	6.53	7.12	7.86	21.2	75	Purple	Water
	$C_{28}H_{40}N_4O_2Br_2Cu\cdot 5H_2O$		(43.22)	(6.48)	(7.20)	(8.17)	(21.03)			
10	CH_3	$-C_6H_4-$[f]	46.92	5.32	7.74	8.71	22.9	82	Brown	Water–acetone
	$C_{28}H_{34}N_4O_2Br_2Cu\cdot 2H_2O$		(46.84)	(5.33)	(7.80)	(8.85)	(22.26)			
11	C_2H_5	$-C_6H_4-$[f]	48.79	6.35	6.63	7.25	18.8	63	Brown	Water–acetone
	$C_{34}H_{56}N_4O_2Br_2Cu\cdot 4H_2O$		(48.72)	(6.49)	(6.68)	(7.58)	(19.06)			
12	*n*-C_3H_7	$-C_6H_4-$[f]	52.00	7.22	6.10	6.43	17.0	90	Brown	Water
	$C_{40}H_{58}N_4O_2Br_2Cu\cdot 4H_2O$		(52.09)	(7.21)	(6.07)	(6.89)	(17.33)			
13	*n*-C_4H_9	$-C_6H_4-$[f]	55.30	7.56	5.57	5.94	15.8	92	Brown	Water–acetone
	$C_{46}H_{70}N_4O_2Br_2Cu\cdot 3.5H_2O$		(55.39)	(7.78)	(5.62)	(6.37)	(16.02)			
14	CH_3	$-C_{10}H_6-$[g]	48.99	5.43	7.05	7.99	19.8	56	Brown	Water
	$C_{32}H_{36}N_4O_2Br_2Cu\cdot 3H_2O$		(48.90)	(5.39)	(7.13)	(8.08)	(20.33)			

a) ( ) represents the calculated value. b) *t*-Butyl groups are attached at 3,3′-positions. c) Cl (%). d) (*R*,*R*)-1,2-Cyclohexylene. e) (*S*,*S*)-1,2-Cyclohexylene. f) 1,2-Phenylene. g) 2,3-Naphthylene.

NaOH solution; then, an aqueous solution (30 cm^3) of KBr (3.1 g, 2.6×10^{-2} mol) was added. When the solution was slowly concentrated to a small volume by evaporating the solvent under a hood, purple (**1**—**8**), green (**9**), or brown (**10**—**14**) crystals were obtained. They were collected by filtration and dried in vacuo. The product was recrystallized from water (**1**,**2**,**8**,**9**,**12**,**14**), or methanol (**3**,**4**,**5**), or by the addition of acetone to the water solution (**6**,**7**,**10**,**11**,**13**). In using 2,3-diaminonaphthalene, the reaction solution was treated under Ar. For **9**, methanol was used as the solvent, and the complex was isolated as chloride, and recrystallized from methanol.

5-(Trimethylammoniomethyl)salicylaldehyde Chloride (15). Trimethylamine gas (0.12 mol) was passed through a stirring tetrahydrofuran solution (50 cm^3) of 5-chloromethylsalicylaldehyde[11] (10 g, 5.9×10^{-2} mol). The thus-formed white precipitate was collected by filtration, washed with ether and dried in vacuo. The crude product was then dissolved in a minimal amount of methanol, and acetone (about 80 cm^3) was added to the solution. After standing for two days, white crystals were obtained, washed with acetone and dried in vacuo. Yield, 10.1 g (63%). ^{1}H NMR (D_2O, TSP (3-(trimethylsilyl)propanesulfonic acid, sodium salt)) δ = 3.11 (s, 9H), 4.51 (s, 2H), 7.15 (d, 1H), 7.75 (d, 1H), 7.93 (s, 1H), 10.02 (s, 1H). Found: C, 57.80; H, 6.79; N, 6.10%. Calcd for $C_{11}H_{16}NO_2Cl$: C, 57.52; H, 7.02; N, 6.10%.

5-(Triethylammoniomethyl)salicylaldehyde Chloride (16). To a stirring tetrahydrofuran (THF) solution (30 cm^3) of 5-chloromethylsalicylaldehyde[11] (7.0 g, 4.1×10^{-2} mol), triethylamine (6.0×10^{-2} mol) diluted with THF (5 cm^3) was slowly added. The white precipitate thus formed was collected by filtration, washed with ether and acetonitrile, and dried in vacuo. The crude product was purified by reprecipitating from methanol–acetone. Yield, 7.3 g (50%). ^{1}H NMR (D_2O, TSP) δ = 1.40 (t, 9H), 3.27 (q, 6H), 4.43 (s, 2H), 7.13 (d, 1H), 7.70 (d, 1H), 7.88 (s, 1H), 10.00 (s, 1H). Found: C, 61.60; H, 7.88; N, 5.03%. Calcd for $C_{14}H_{22}NO_2Cl$: C, 61.87; H, 8.16; N, 5.15%.

5-(Tripropylammoniomethyl)salicylaldehyde Chloride (17). The crude product of **17** was obtained by a similar method to that of **16**, recrystallized from methanol and dried in vacuo. Yield, 45%. ^{1}H NMR (D_2O, TSP) δ = 1.00 (t, 9H), 1.87 (m, 6H), 3.12 (t, 6H), 4.49 (s, 2H), 7.15 (d, 1H), 7.67 (d, 1H), 7.82 (s, 1H), 10.00 (s, 1H). Found: C, 63.98; H, 8.95; N, 4.52%. Calcd for $C_{17}H_{28}NO_2Cl\cdot 0.25H_2O$: C, 64.13; H, 9.02; N, 4.40%.

5-(Tributylammoniomethyl)salicylaldehyde Chloride (18). The crude product of **18** was obtained by a similar method to that of **16**. It was recrystallized from water and dried in vacuo. Yield, 56%. ^{1}H NMR (D_2O, TSP) δ = 1.00 (t, 9H), 1.40 (m, 6H), 1.82 (m, 6H), 3.18 (t, 6H), 4.50 (s, 2H), 7.18 (d, 1H), 7.70 (d, 1H), 7.82 (s, 1H), 10.01 (s, 1H). Found: C, 60.99; H, 9.30; N, 3.54%. Calcd for $C_{20}H_{34}NO_2Cl\cdot 2H_2O$: C, 61.28; H, 9.77; N, 3.57%.

3-*t*-Butyl-5-(trimethylammoniomethyl)salicylaldehyde Chloride (19). This compound was obtained as a white powder by the reaction of 3-*t*-butyl-5-chloromethylsalicylaldehyde (**20**) with trimethylamine in THF. Yield, 76%. ^{1}H NMR of **19** (D_2O, TSP) δ = 1.40 (s, 9H), 3.10 (s, 9H), 4.48 (s, 2H), 7.69 (s, 1H), 7.78 (s, 1H), 9.90 (s, 1H). Found for **19**: C, 57.52; H, 8.74; N, 4.63%. Calcd

for $C_{15}H_{24}NO_2Cl \cdot 1.5H_2O$: C, 57.60; H, 8.70; N, 4.48%. **20** was prepared by the chloromethylation of 3-*t*-butylsalicylaldehyde[12] using the method of Angyal et al.[11] Yield, 52%.

Materials. All of the reagents and solvents used were of analytical grade. Ethylenediamine, 1,3-diaminopropane, 1,2-diaminocyclohexane, 1,2-phenylenediamine, and 2,3-diaminonaphthalene were purchased from commercial sources. (*R*,*R*)- and (*S*,*S*)-1,2-diaminocyclohexanes were obtained by a reference methods.[13] 2,3-Dimethyl-2,3-diaminobutane was prepared by a method of Sayre.[14] Dojin Chemical buffer HEPES (3-[4-(2-hydroxyethyl)-1-piperazinyl]propanesulfonic acid) was purchased from commercial sources and used without purification. Calf thymus DNA, poly(dA-dT)–poly(dA-dT), poly(dG-dC)–poly(dG-dC), poly(dA-dC)–poly(dT-dG) were purchased from Merck Co., Ltd., and the calf thymus DNA was used after purification.

Measurements. UV-vis and CD spectra were recorded on a Shimadzu UV-2200 spectrophotometer and JASCO J-720 spectropolarimeter at 25.0 °C, respectively. IR spectra were measured with a JASCO FT/IR-300E. ^{1}H NMR and EPR spectra were recorded on a JEOL GSX-400 spectrometer (400 MHz) and a JEOL FE2XG, respectively. The magnetic susceptibility was measured with a Shimadzu Torsion Magnetometer MB-100 by the Faraday method at room temperature. The electronic conductivity was measured with a Radiometer Copenhagen CDM 92 for 1×10^{-4} M (M = mol dm^{-3}) complex solutions at 25 °C. CHN elemental analysis was carried out with a Yanaco MT-5. Cu was analyzed with a Hitachi atomic absorption spectrophotometer 170-30. Br was analyzed by the Mohr method.

X-Ray Crystal Structure Analysis. A purple crystal of **1** was used for data collection. The lattice parameters and intensity data were measured on a Rigaku diffractometer (AFC-7R) with graphite-monochromated Mo $K\alpha$ radiation and a 12 kW rotating-anode generator. The structure was solved by a direct method. The nonhydrogen atoms were refined anisotropically, and the hydrogen atoms were refined isotropically. The final cycle of a full-matrix least refinement was 7468 observed reflections ($I>3.00\sigma(I)$). All of the calculations were performed using the TEXSAN crystallographic software package developed by Molecular Structure Corporation (1985).

Conditional Stability Constants of the Complexes. To a solution containing a Schiff base complex (1.0×10^{-5} M) and HEPES (5.0 mM, pH 7.2), a solution of EDTA·2Na (1.0×10^{-5} M) was added; the absorption spectra of the solutions were followed at 25 °C until the ligand substitution equilibrium was achieved (10 days). The conditional stability constants of the Schiff base complexes were calculated using the concentrations of the complexes (Cu-Schiff base and Cu-edta^{2-}) and free ligands, which were estimated from the absorbance (340 nm for **1** and 400 nm for **10**,**12**,**14**) of the solutions at the equilibium conditions, the stability constant of Cu-edta^{2-}, and the deprotonation constant of EDTA.[15]

Aggregation Constants. The absorption spectra were measured for solutions containing complex concentrations ranging from 1×10^{-4} to 1×10^{-2} M at 25 °C, and the aggregation constants K_{dimer} (K_{dimer} = [dimer]/[monomer]^2) were estimated from the absorbance at 555 nm by applying reference methods.[16]

Equilibirium Dialysis. A typical example is described. The retentates (5.0 cm^3) containing a solution of 100 μM complex, 5.0 mM HEPES buffer, 50 mM NaCl, and calf thymus DNA (0—1000 μM) were dialyzed against 15.0 cm^3 dialysates containing a solution of 5.0 mM HEPES (pH = 7.2) and 50 mM NaCl using a dialysis membrance (Size 16, Wako Pure Chemical Industries Ltd.) for 48 h, after which time equilibrium was achieved. The temperature was held at 25 °C and the samples were shaken at a constant rate. Upon equilibration, dialysates were subjected to spectral analysis and the concentrations of the free complex were determined on the basis of absorbance readings at 342 nm (**1**,**7**,**8**), 343 nm (**2**,**3**,**6**), 345 nm (**9**), 346 nm (**4**), 352 nm (**5**), and 395 nm (**11**—**13**). In the case of complexes **10** and **14**, precipitation ocurred during dialysis. The obtained data were conducted to a macroscopic analysis of the binding constants. In addition to these experiments, the dialysis of a solution containg a constant concentration of DNA base pairs (2.0×10^{-4} M for typical example) and varying complex concentrations (2.5×10^{-5}—2.5×10^{-4} M for typical example) was also performed for all of the complexes; however, precipitation ocurred during the dialysis for **2**—**10**, and **14**. The data for **1** and **11**—**13** were used in a microscopic analysis of the binding constants.

UV-vis and CD Titrations. A typical method is described. The solutions containing the complexes, DNA, 5.0 mM HEPES buffer (pH = 7.2), and 50 mM NaCl were made and the UV-vis and CD spectra were measured after 24 h mixing at 25 °C using 1 cm cell (UV-vis) and 5 cm cell (CD). For AT-DNA, GC-DNA, and ACTG-DNA, 1 cm semi-microcell was used. The complex concentrations were 4×10^{-5} M for **1**—**9**, 2×10^{-5} M for **10**—**13**, and 1×10^{-5} M for **14**. The DNA base pair concentration was 0—1×10^{-3} M for **1**—**9**, 0—2×10^{-4} M for **10**—**13**, and 0—8×10^{-5} M for **14**. The UV-vis and CD spectral data were used in a macroscopic analysis of the binding constants. The wavelength for absorbance readings was the same as that for equilibrium dialysis. The reading wavelengths for CD titration were as follows: 365 nm (**1**,**6**,**7**), 380 nm (**2**—**4**), 385 nm (**5**,**8**,**9**,**10**—**13**), 430 nm (**14**), and 450 nm (**10**). For a microscopic analysis, a solution containing a constant concentration of DNA base pairs (4.2×10^{-5} M for typical example) and varying concentrations of the complex (8.0×10^{-6}—3.5×10^{-5} M for typical case) was prepared.

Analysis of Binding Constants with DNA. In this paper, the concentration of DNA base pairs was used as the concentration of DNA. The binding constants (K_b) of the complexes with calf thymus DNA were estimated by applying two methods, macroscopic and microscopic analysis.[17] For poly(dA-dT)–poly(dA-dT), poly(dG-dC)–poly(dG-dC), and poly(dA-dC)–poly(dT-dG), macroscopic analysis was applied.

For a macroscopic analysis, K_b is defined by Eq. 1 and was estimated by applying Eq. 2:

$$\mathrm{M} + \mathrm{DNA} \rightleftarrows \mathrm{M\text{-}DNA};\quad K_b = [\mathrm{M\text{-}DNA}]/([\mathrm{M}][\mathrm{DNA}]) \tag{1}$$

$$C_M/C_B = (K_b C_D)^{-1} \tag{2}$$

where M denotes a free metal complex, and C_B, C_M, and C_D represent the concentrations of M-DNA, free metal complex, and free DNA base pairs, respectively. The stepwise equilibrium constants (K_{b1} and K_{b2}) are defined by Eqs. 3 and 4, respectively, and were calculated using Eqs. 5 and 6:

$$\mathrm{M} + \mathrm{DNA} \rightleftarrows \mathrm{M\text{-}DNA};\quad K_{b1} = [\mathrm{M\text{-}DNA}]/([\mathrm{M}][\mathrm{DNA}]) \tag{3}$$

$$\mathrm{M} + \mathrm{M\text{-}DNA} \rightleftarrows \mathrm{M_2\text{-}DNA};\quad K_{b2} = [\mathrm{M_2\text{-}DNA}]/([\mathrm{M}][\mathrm{M\text{-}DNA}]) \tag{4}$$

$$K_{b1}^2 = K_{b3}K_{b4}, \tag{5}$$

$$K_{b2}^2 = K_{b3}/K_{b4}, \tag{6}$$

where K_{b3} and K_{b4} are the equilibrium constants defined by Eqs. 7 and 8, respectively:

$$2\mathrm{M} + \mathrm{DNA} \rightleftarrows \mathrm{M_2\text{-}DNA};\ K_{b3} = [\mathrm{M_2\text{-}DNA}]/([\mathrm{M}]^2[\mathrm{DNA}]) \tag{7}$$

M_2-DNA + DNA $\rightleftarrows$ 2M-DNA;

$$K_{b4} = [\text{M-DNA}]^2/([M_2\text{-DNA}][\text{DNA}]). \quad (8)$$

Eqs. 7 and 8 correspond to the DNA titrations for a low R (R= $[\text{DNA}]_{total}/[\text{M}]_{total}$) and a high R, respectively. The K_{b3} and K_{b4} were estimated by applying Eqs. 9 and 10, respectively:

$$C_M{}^2/C_{B2} = (K_{b3}C_D)^{-1}, \quad (9)$$

$$C_{B2}/C_B{}^2 = (K_{b4}C_D)^{-1}, \quad (10)$$

where C_{B2} indicates the concentration of M_2-DNA. Experiments for a macroscopic analysis were carried out under a constant complex concentration and varing DNA base pairs concentration.

For a microscopic analysis, a Scatchard plot was carried out applying Eq. 11:[17]

$$C_B/([\text{DNA}]_tC_M) = K_b/n - K_bC_B/[\text{DNA}]_t \quad (11)$$

where $[\text{DNA}]_t$ and n mean the total concentration of DNA base pairs and site size base pairs, respectively. The experiments for a microscopic analysis were carried out under a constant concentration of DNA base pairs and a varing complex concentration.

Results and Discussion

Preparation and Properties of the Complexes. All of the cationic Schiff base complexes of copper(II) were prepared in "one-pot" by reacting 5-(trialkylammoniomethyl)-salicylaldehyde chloride with copper(II) acetate and diamine in a 2 : 1 : 1 molar ratio in water at pH 7.4, and isolated as bromide salt, except for complex **5**. In the case of **5**, methanol was used as the solvent and the chloride salt was isolated. The data of the elemental analysis and the purification method of the complexes are summarized in Table 1. All of the complexes could also be isolated as tetrafluoroborate, perchlorate, and chloride salts. However, the former two salts were miserably soluble in water and the chloride salt was hygroscopic. All of the bromide salts were very soluble in water and methanol, and the electronic conductivity in water corresponded to 1 : 2 electrolyte (Table 2).

All of the complexes prepared here were thermally stable in the atmosphere and in water (pH=7.2) even at 80 °C. However, the Schiff base ligands, themselves, were thermally unstable in water and methanol; although the formation of the Schiff base ligands was confirmed from the UV-vis spectra, the ligands gradually decomposed to form insoluble yellow products when heated. The products were presummed to be a Hoffman-type decomposition product ($(H_2C{=}C_6H_2(=O)\text{–}CH{=}N)_2$–X, X=bridging group) of the cationic Schiff base ligands on the basis of an elemental analysis and the IR spectra of the products. 5-(Trialkylammoniomethyl)salicyladehyde chloride was also thermally not so stable in water; it gradually decomposed to form an insoluble white product when heated.

Characterization of the Complexes. The characterization data are listed in Table 2. All of the complexes show $\nu_{C=N}$ at 1615—1640 cm^{-1} and ν_{C-O} at 1525—1540 cm^{-1}, which are characteristic to Cu(II)-Schiff base complexes.[17] The strong ν_{C-H} bands at 2850—2930 cm^{-1} are due to the trialkyl group. All of the complexes show d–d transition bands at 17000—18000 cm^{-1}, CT bands at 24500—33000 cm^{-1}, and π–π^* bands at 37400—41600 cm^{-1} in water, which are very similar to those of the non-charged Cu(II)-Schiff base complexes having a square-planar structure.[18,19] The CD spectra of **8** and **9** are comparable to those of [Cu(salchxn)].[19] The magnetic moments (1.82—1.89 BM) and $g_{\|}$-values (2.207—2.218) well correspond to those of copper(II)-Schiff base complexes having a square-planar N_2O_2 geometry.[18] Accordingly, these data in Table 2 clearly indicate that the prepared cationic Schiff base complexes had a quite similar structure to that of the corresponding non-charged Schiff base complexes of copper(II), and that the trialkylammoniomethyl groups had little influenced on the Cu(II)-Schiff base skeleton. In the case of **10**—**14**, the EPR spectra in frozen water exhibit strong triplet signals due to the dimer overlapped with those corresponding to the monomer, indicating that the complexes with an aromatic *N,N'*-bridging group aggregate in solution.

Crystal Structure of the Complex 1. Figure 1 shows an ORTEP drawing of complex **1** with 50% probability thermal ellipsoids. The selected crystal data and collection parameters are summarized in Table 3. The atomic parameters are listed in Table 4. The selected bond distances and bond angles are given in Tables 5 and 6. The complete $F_o - F_c$ data are deposited as Document No. 70006 at the Office of the Editor of Bull. Chem. Soc. Jpn. The Cu(II) ion is surrounded in a square-planar geometry by two nitrogen and two oxygen atoms of the Schiff base ligand. The bond distances of Cu–N (1.938 Å, 1.934 Å) and Cu–O (1.903 Å, 1.903 Å) and the bond angles around the Cu atom are close to those of [Cu(salen)].[19] Further, the bond distances and bond angles for the salen skeleton are also very similar to those of [Cu-(salen)], indicating that the coordination structure of cationic Schiff base complexes is essentially the same as that of a non-charged one. The trimethylammoniomethyl groups are

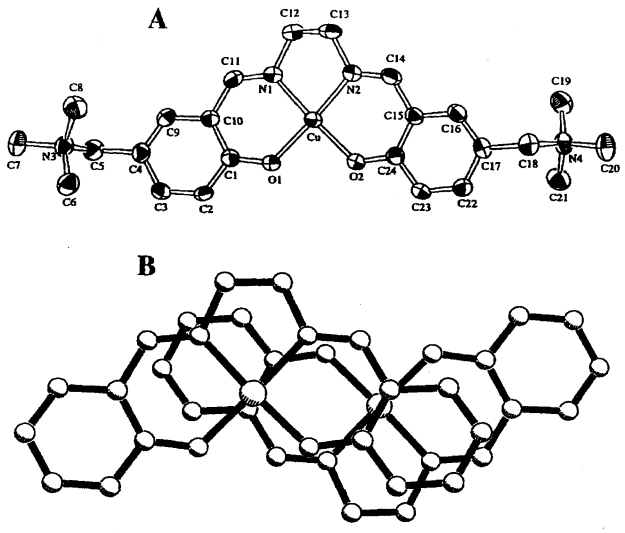

Fig. 1. **A**: ORTEP drawing of cationic part of complex **1** with 50% probability thermal ellipsoids. **B**: Dimer structure of **1** viewed perpendicular to the mean plane (the trimetylammoniomethyl groups are omitted).

Table 2. Characterization Data of the Complexes

Complex	Λ_M in waer	IR/cm^{-1} in KBr			UV-vis in water	μ_{corr}	ESR[a]	
	S cm^2 mol^{-1}	ν_{C-H}	$\nu_{C=N}$	ν_{C-O}	$\tilde{\nu}$/cm^{-1} (ε/mol^{-1}dm^{3}cm^{-1})	B.M.	$g_{\parallel}$	$\frac{\lvert A_{\parallel}\rvert}{\text{cm}^{-1}}$
1	185	2920-2860	1640	1535	17650 (270), 29120 (8720), 37630 (29900sh) 41250 (68800)	1.89	2.214	0.0201
2	198	2920 2850	1635	1535	17660 (270), 29120 (8800), 37590 (29700sh) 41250 (68400)	1.88	2.216	0.0197
3	195	2940 2870	1635	1535	17660 (280), 29120 (9000), 37410 (31000sh) 41150 (71700)	1.86	2.217	0.0194
4	187	2930 2870	1630	1535	17660 (280), 29060 (9000), 37700 (31000sh) 41190 (69700)	1.85	2.214	0.0195
5	211	2940 2860	1630	1535	17750 (290), 28430 (9690), 40420 (54600) 42500 (42400sh)	1.87	2.209	0.0196
6	297	2920 2850	1620	1540	18140 (260), 29180 (9890), 37570 (29800sh) 41390 (76100)	1.84	2.205	0.0202
7	217	2920 2860	1620	1535	16850 (190), 29890 (8930), 36820 (19300sh) 41630 (67300), 43760 (56100sh)	1.87	2.248	0.0184
8	191	2920 2860	1630	1540	17760 (230), 29220 (8960), 37400 (26600sh) 41425 (69980) [16260 (−0.26), 20000 (0.75), 27778 (−12.3) 30120 (5.18), 41152 (−55.5), 44247(36.7) 49019 (−9.70)][c]	1.83	2.214	0.0197
9	187	2920 2860	1630	1540	17760 (230), 29220 (8960), 37400 (26600sh) 41425 (70000) [16260 (0.26), 20000 (−0.75), 27778 (12.3) 30120 (−5.18), 41152 (55.5), 44247 (−36.6) 49019 (9.70)][c]	1.83	2.218	0.0191
10	210	2920 2850	1620	1530	18070 (310), 25280 (17700), 30080 (18500) 32950 (23500), 39760 (52800)	1.82	2.211[b]	0.0203
11	192	2920 2850	1620	1530	17950 (290), 25190 (17900), 30030 (19200) 33000 (24300), 39920 (53200)	1.82	2.213[b]	0.0202
12	187	2930 2880	1620	1530	18060 (300), 25160 (16900), 29990 (18300) 32950 (22900), 39760 (50800)	1.82	2.207[b]	0.0204
13	190	2930 2870	1615	1525	18010 (330), 25160 (17800), 29990 (19400) 32890 (24300), 39760 (53500)	1.86	2.209[b]	0.0202
14	198	2920 2850	1620	1535	16950 (190), 24660 (18000), 31700 (20800) 40320 (48700)	1.82	b)	

a) Frozen water containing 20% ethylene glycol. b) Overlap with triplet peaks due to dimer. c) CD extrema ($\tilde{\nu}$/cm^{-1} ($\Delta\varepsilon$/mol^{-1} dm^3 cm^{-1})) in water.

attached in a *trans* form with respect to the plane of the Cu-salen skeleton.

Complex **1** exists as loosely held dimers in a crystal (Fig. 1B). Although the dimeric face-to-face structure resembles that of [Cu(salen)],[20] the face-to-face atoms are clearly different from those of [Cu(salen)]. That is, although the Cu atom of **1** faces the C(10) atom at an intermolecular distance of 3.40 Å, the Cu atom of [Cu(salen)] faces the phenolic oxygen atom at an intermolecular distance of 2.41 Å. If **1** takes the same dimer structure as [Cu(salen)], the trimethylammoniomethyl groups of **1** are face-to-face to each other, so that **1** takes a somewhat slide-dimer structure in order to avoid a steric and/or electrostatic repulsion(s) among the trimethylammoniomethyl groups.

Stability for Ligand-Substitution of the Complexes. It is an important factor in the determination of the binding constants with DNA that the complexes have a substantial stability for ligand-substitution. Thus, we tested the stability of the following representative complexes: **1**,**10**,**12**, and **14**. The complexes (1.0×10^{-5} M) showed no spectral change upon the addition of pyridine (5.0×10^{-4} M), ammonia (5.0×10^{-4} M), Na_2HPO_4 (5.0×10^{-2} M), and HEPES buffer (5.0×10^{-2} M). In the addition of EDTA·2Na (1.0×10^{-5} M), about a 10% decoloration of the Schiff base complexes was observed under the equilibrium conditions at pH 7.2 (HEPES). Based on the spectral change, the conditional stability constants (K_{app}=[complex]/[Cu^{2+}][total free ligand])) were estimated to be approximately 2×10^{14} M^{-1} at pH 7.2 (Table 7). These data indicate that the cationic Schiff base complexes have a substantial stability at pH 7.2, and that the dissociation of the complexes can be safely neglected under the experimental conditions for the DNA-binding constants (complex concentrations=1—40×10^{-5} M pH 7.2).

Aggregation of the Complexes in Water. It has been reported that the non-charged salen-type Shiff base complexes of copper(II) often exists as a dimer in the solid state.[20—22]

Table 3. Crystal Data and Data Collection Details

Formula	$C_{24}H_{44}N_4O_7Br_2Cu$
Formula weight	723.99
Crystal system	Triclinic
Space group	$P\bar{1}$
a/Å	11.087(1)
b/Å	14.993(1)
c/Å	9.937(2)
α/deg	95.16(1)
β/deg	106.70(1)
γ/deg	77.793(8)
V/Å^3	1545.5(3)
Z	2
d(calcd)/g cm^{-3}	1.556
Crystal size/mm^3	0.43×0.43×0.40
t/°C	23±1
Radiation	Mo $K\alpha$
	λ=0.71069 Å
μ/cm^{-1}	33.5
Scan mode	ω–2θ
Scan width/deg	1.73+0.30 tan θ
Scan speed/deg min^{-1}	16.0
2θ range	39.04–39.96°
No. of measured reflections	7468
No. of observed reflections	4453
R/%	3.4
R_w/%	3.7

The dimer partly monomerizes in the non-coordinating solvent, while the equilibrium largely shifts to the monomer in the coordinating solvents.[23] In the case of cationic Shiff base complexes, complexes **1**—**9** show an EPR corresponding to only one monomer species in a frozen aqueous solution. Complexes **10**—**14**, however, exhibit strong triplet signals due to the dimer species overlapped with those corresponding to the monomer (Table 2). As listed in Table 7, the formation constant (K_{dimer}) of the dimer increases in the order **1**≪**12**<**10**<**14**, indicating that the dimer formation is enhanced along with an increase in the hydrophobicity of the *N*,*N*′-bridging group of the complexes. On the other hand, the K_{dimer} values are in the range of 2.3—5.3×10 M^{-1}, which show that the concentration of the dimer is negligibly small in the complex concentrations (1—20×10^{-5} M) adopted to measure the DNA-binding constants.

UV-vis and CD Titrations. No color from the complexes remained in the supernatant solution obtained after ultracentrifugation of a solution of calf thymus DNA and complexes (R=[DNA]$_{total}$/[M]$_{total}$=20), indicating that all of the complexes bind strongly to DNA. The complexes were thermodynamically so stable that no ligand substitution nor a formation of mixed-ligand complex occured upon the addition of NH_3 (5×10^{-4} M), pyridine (5×10^{-4} M), and phosphate ion (5×10^{-2} M) to the complex solutions (1×10^{-5} M). This fact indicates that the possibility of coordination binding between the complexes and DNA can be excluded. As reported previously,[10] the ESR study for complex-bind-

Table 4. Atomic Coordinates and Equivalent Isotropic Thermal Parameters

Atom	x	y	z	B_{eq} [a]
Br(1)	0.19934(4)	0.38317(3)	0.20846(5)	5.45(1)
Br(2)	0.70543(4)	0.31389(3)	0.12971(4)	4.77(1)
Cu(1)	0.67410(4)	0.03163(3)	0.45881(4)	2.573(8)
O(1)	0.6417(2)	0.0662(1)	0.6362(2)	2.82(5)
O(2)	0.8286(2)	−0.0477(1)	0.5511(2)	3.07(5)
O(3)	0.5215(4)	0.3534(5)	0.3581(5)	10.7(2)
O(4)	1.0147(3)	0.3580(3)	0.4125(4)	6.40(9)
O(5)	0.1210(3)	0.0483(2)	0.1551(3)	5.48(7)
O(6)	0.1745(4)	0.1922(3)	0.0253(3)	7.6(1)
O(7)	0.8602(3)	0.1143(3)	1.0121(4)	6.81(9)
N(1)	0.5113(3)	0.1024(2)	0.3555(3)	3.34(6)
N(2)	0.7068(2)	0.0103(2)	0.2765(3)	2.87(6)
N(3)	0.2465(2)	0.4124(2)	0.7916(3)	3.11(6)
N(4)	1.2276(2)	−0.3392(2)	0.2900(3)	3.08(6)
C(1)	0.5433(3)	0.1233(2)	0.6599(3)	2.42(6)
C(2)	0.5425(3)	0.1470(2)	0.7999(3)	2.84(7)
C(3)	0.4429(3)	0.2063(2)	0.8337(3)	3.07(7)
C(4)	0.3362(3)	0.2481(2)	0.7299(3)	2.88(7)
C(5)	0.2273(3)	0.3137(2)	0.7667(4)	3.28(8)
C(6)	0.3597(4)	0.4210(3)	0.9132(5)	3.95(10)
C(7)	0.1294(4)	0.4698(3)	0.8246(5)	4.16(10)
C(8)	0.2632(5)	0.4474(3)	0.6636(4)	4.3(1)
C(9)	0.3336(3)	0.2260(2)	0.5927(3)	2.94(7)
C(10)	0.4347(3)	0.1656(2)	0.5536(3)	2.60(6)
C(11)	0.4249(3)	0.1509(2)	0.4064(3)	3.31(7)
C(12)	0.4870(4)	0.0893(3)	0.2027(4)	5.5(1)
C(13)	0.6094(4)	0.0664(3)	0.1679(4)	4.46(9)
C(14)	0.8042(3)	−0.0411(2)	0.2490(3)	3.26(8)
C(15)	0.9118(3)	−0.0921(2)	0.3501(3)	2.67(7)
C(16)	1.0145(3)	−0.1410(2)	0.3011(3)	3.00(7)
C(17)	1.1236(3)	−0.1889(2)	0.3885(3)	2.92(7)
C(18)	1.2344(3)	−0.2396(2)	0.3362(4)	3.24(8)
C(19)	1.1229(4)	−0.3435(3)	0.1584(4)	4.06(9)
C(20)	1.3533(4)	−0.3830(3)	0.2623(5)	4.8(1)
C(21)	1.2074(4)	−0.3892(3)	0.4021(4)	4.08(9)
C(22)	1.1313(3)	−0.1859(2)	0.5320(3)	3.20(7)
C(23)	1.0337(3)	−0.1394(2)	0.5835(3)	3.32(8)
C(24)	0.9193(3)	−0.0910(2)	0.4953(3)	2.71(7)

a) $B_{eq}=(8\pi^2/3)\sum_i\sum_j U_{ij}a_i^*a_j^*\boldsymbol{a}_i\cdot\boldsymbol{a}_j$.

Table 5. Selected Bond Distances (Å)

Cu–N(1)	1.939(3)	Cu–N(2)	1.934(3)
Cu–O(1)	1.904(2)	Cu–O(2)	1.903(2)
N(1)–C(11)	1.273(4)	N(2)–C(14)	1.271(4)
N(1)–C(12)	1.467(4)	N(2)–C(13)	1.466(4)
O(1)–C(1)	1.302(3)	O(2)–C(24)	1.311(4)
N(3)–C(5)	1.528(4)	N(4)–C(18)	1.533(4)
N(3)–C(6)	1.491(4)	N(4)–C(19)	1.489(4)
N(3)–C(7)	1.502(4)	N(4)–C(20)	1.500(5)
N(3)–C(8)	1.492(4)	N(4)–C(21)	1.485(5)
C(4)–C(5)	1.499(4)	C(17)–C(18)	1.502(4)
C(10)–C(11)	1.436(4)	C(14)–C(15)	1.443(4)
C(12)–C(13)	1.460(6)		

Estimated standard deviations are given in parentheses.

Table 6. Selected Bond Angles (°)

N(1)–Cu–N(2)	84.2(1)	O(1)–Cu–O(2)	89.45(8)
O(1)–Cu–N(1)	93.11(10)	O(2)–Cu–N(2)	93.69(10)
O(1)–Cu–N(2)	173.81(10)	O(2)–Cu–N(1)	174.6(1)
Cu(1)–O(1)–C(1)	127.2(2)	Cu–O(2)–C(24)	126.9(2)
Cu(1)–N(1)–C(12)	113.0(2)	Cu–N(2)–C(13)	112.6(2)
Cu(1)–N(1)–C(11)	127.1(2)	Cu–N(2)–C(14)	126.4(2)
C(11)–N(1)–C(12)	119.7(3)	C(13)–N(2)–C(14)	120.8(3)
N(1)–C(11)–C(10)	125.0(3)	N(2)–C(14)–C(15)	125.5(3)
N(1)–C(12)–C(13)	109.2(3)	N(2)–C(13)–C(12)	110.6(3)
N(3)–C(5)–C(4)	114.5(3)	N(4)–C(18)–C(17)	114.5(3)
C(5)–N(3)–C(6)	111.4(3)	C(18)–N(4)–C(19)	110.4(3)
C(5)–N(3)–C(7)	108.1(3)	C(18)–N(4)–C(20)	107.4(3)
C(5)–N(3)–C(8)	110.7(3)	C(18)–N(4)–C(21)	111.0(3)
C(6)–N(3)–C(7)	108.3(3)	C(19)–N(4)–C(20)	109.1(3)
C(6)–N(3)–C(8)	109.4(3)	C(19)–N(4)–C(21)	110.0(3)
C(7)–N(3)–C(8)	108.9(3)	C(20)–N(4)–C(21)	108.9(3)

Estimated standard deviations are given in parentheses.

Table 7. Conditional Stability Constants (K_{app}) and Dimer-Formation Constants (K_{dimer}) at 25 °C

Complex	K_{app}/M^{-1} a)	K_{dimer}/M^{-1}
1	1.6×10^{14}	0
10	2.5×10^{14}	35
12	2.3×10^{14}	23
14	2.2×10^{14}	53

a) HEPES=5.0 mM (pH=7.2).

ing DNA-fiber indicates that complexes **1** and **6** selectively bind to the groove of DNA, whereas **10**—**14** selectively intercalate to the base pairs of DNA. These facts suggest that the salen-type Shiff base complexes of copper(II) have a high mode selectivity depending on the nature of the *N,N'*-bridging group of the Schiff base ligand. In order to confirm the mode selectivity and to obtain further information, we investigated the UV-vis and CD spectral behaviors of **1**—**14** in the DNA solution. The UV-vis and CD spectra were measured under a constant complex concentration and varing DNA base-pair concentration. The typical spectra are shown in Figs. 2, 3, 4, 5, and 6.

As a result, although complexes **1**—**9**, which have an aliphatic *N,N'*-bridging group, showed no clear UV-vis spectral change under the employed experimental conditions, they exhibited clear induced CD spectra (**1**—**7**) or a red shift of the CD spectra (**8**,**9**) ar the CT band region (300—500 nm) (Figs. 2 and 3). The slight UV-vis spectral change strongly suggests that the compelxes bind at the surface or the groove of the double helix of DNA, because the surface binding and groove binding usually have little effect on the absorption spectra of metal complexes.[1b] The relatively strong induced CD of **1**—**7** and the red shift of the CD of **8** and **9** suggest that the binding mode is groove binding, rather than surface binding, because the latter process would be expected to be nonspecific regarding the orientation of the complexes, whereas the CD spectra attest that the binding is geometrically homogenious to some extent. In fact, we have

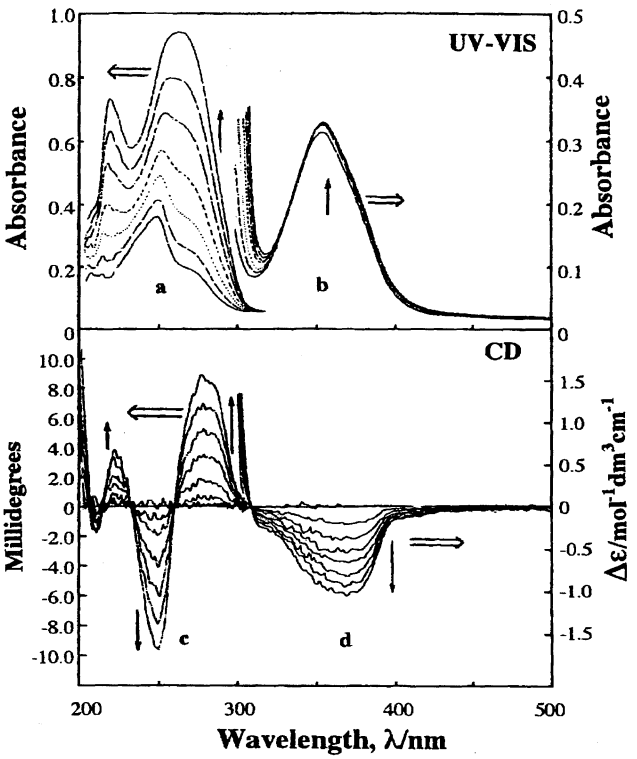

Fig. 2. UV-vis and CD spectral variations of complex **1** by the addition of calf thymus DNA. **a**: [Complex]=5.0×10^{-6} M, [DNA]=0—8.4×10^{-5} M, Cell length=1.0 cm. **b**: [Complex]=4.0×10^{-5} M, [DNA]=0—9.9×10^{-4} M, Cell length=1.0 cm. **c**: [Complex]=4.0×10^{-5} M, [DNA]=0—6.7×10^{-4} M, Cell length=0.1 cm. **d**: [Complex]=4.0×10^{-5} M, [DNA]=0—9.9×10^{-4} M, Cell length=5.0 cm. I=0.05 (50 mM NaCl+5 mM HEPES (pH=7.2)). T=25°C. $\Delta\varepsilon$ value is plotted per mol dm^{-3} of complex.

observed that about 75% of **1** is oriented to take a dihedral angle of 30°±10° between the coordination plane of **1** and the DNA helix axis in the solid state.[10]

The induced CD's at the CT band region of **1**—**7** comprise two main CD bands. The CD sign is (−),(−) from the shorter to longer wavelength for **1**; (−),(+) for **2**—**5**; and (+),(−) for **6** and **7**. Since the induced CD spectra of **2**—**5** are very similar to the CD spectrum of optically active **9**, **2**—**5** are assumed to be oriented in such a way that the coordination plane of these complexes is tetrahedrally distoreted to take a *Δ* configuration, because **9** has been known to take stereospecifically the *Δ* configuration.[19] This assumption is partly supported by the fact that the CD intensity of **9** is scarecely changed by the addition of DNA. Similary, the induced CD spectra of **6** and **7** are very similar to the CD spectrum of **8**, they are assummed to take a *Λ* configuration. Also in this case, the CD intensity of **8** is scarecely changed by the addition of DNA. The induced CD of **1** is different from the CD spectra of **8** and **9**. Since the CD intensity is two- or three-times stronger than those of **2**,**3**, and **4**, which have a similar structure to **1**, it is suggested that the effect of an asymmetric electronic field and an asymmetric magnetic field of chiral DNA affects the induced CD of **1** in addition to the effect of

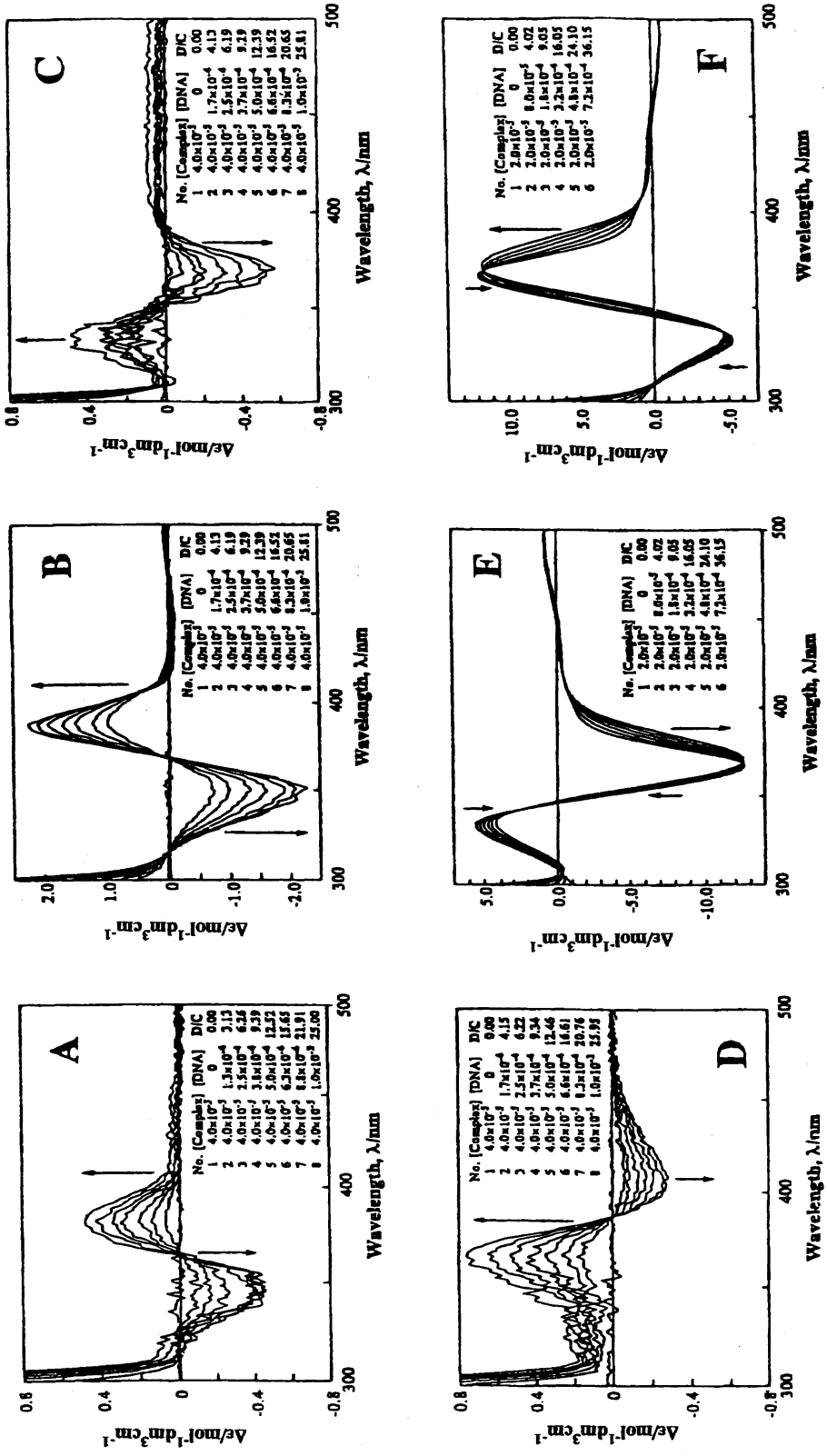

Fig. 3. CD spectral variations by the addition of calf thymus DNA. **A**: complex **2**, **B**: complex **5**, **C**: complex **6**, **D**: complex **7**, **E**: complex **8**, **F**: complex **9**. [Complex]=4.0×10^{-5} M for **A**—**D** and 2.0×10^{-5} M for **E** and **F**. [DNA]=0—1.0×10^{-3} M for **A**—**D** and 0—7.2×10^{-4} M for **E** and **F**. I=0.05 (50 mM NaCl+5 mM HEPES (pH=7.2)). T=25°C. $\Delta\varepsilon$ value is plotted per mol dm^{-3} of complex. The CD spectral variations of complexes **3** and **4** (not drawn) are close to that of **2**.

a distortion of the coordination plane.[24] Recently, a similar effect to this was reported for the induced CD of salen-type Schiff base complexes of copper(II) with a cationic group at the *N*,*N*′-bridging group.[9f]

DNA solutions containing **1**—**9** show CD with opposite signs at near 260 nm, indicating that the DNA keeps the double helix B-form structure in the presence of **1**—**9**.[25] The presence of iso-CD point(s) in the CT band region for **2**—**9** indicates that the reaction with DNA can be treated as the following equilibrium:

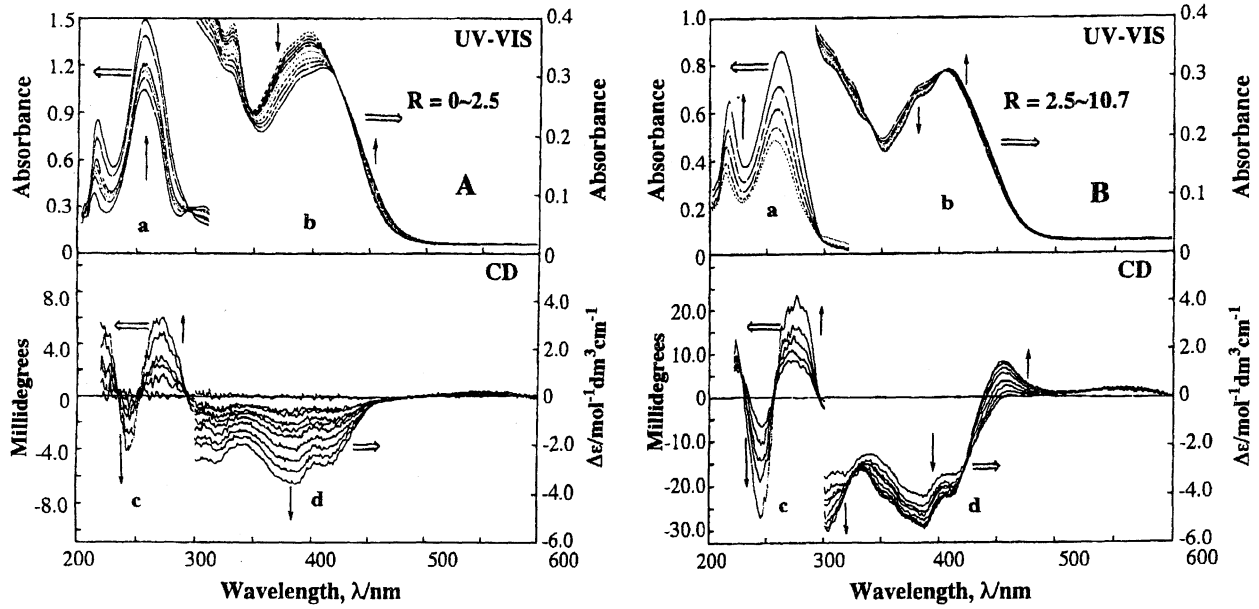

Fig. 4. UV-vis and CD spectral variations of complex **10** by the addition of calf thymus DNA. **A**: R=0—2.4. [Complex]=2.0×10^{-5} M. [DNA]=0—3.9×10^{-5} M for **a** and **c**, 0—4.7×10^{-5} M for **b** and **d**. Cell length=1.0 cm for **a** and **b**, 0.1 cm for **c**, and 5.0 cm for **d**. **B**: R=2.5—10.7. [Complex]=5.0×10^{-6} M for **a**, 2.0×10^{-5} M for **b**, **c**, and **d**. [DNA]=(1.5—4.0)$\times10^{-5}$ M for **a**, (5.9—21)$\times10^{-5}$ M for **b** and **d**, (5.9—16)$\times10^{-5}$ M for **c**. Cell length=1.0 cm for **a** and **b**, 0.1 cm for **c**, and 5.0 cm for **d**. I=0.05 (50 mM NaCl+5 mM HEPES (pH=7.2)). T=25°C. $\Delta\varepsilon$ value is plotted per mol dm^{-3} of complex.

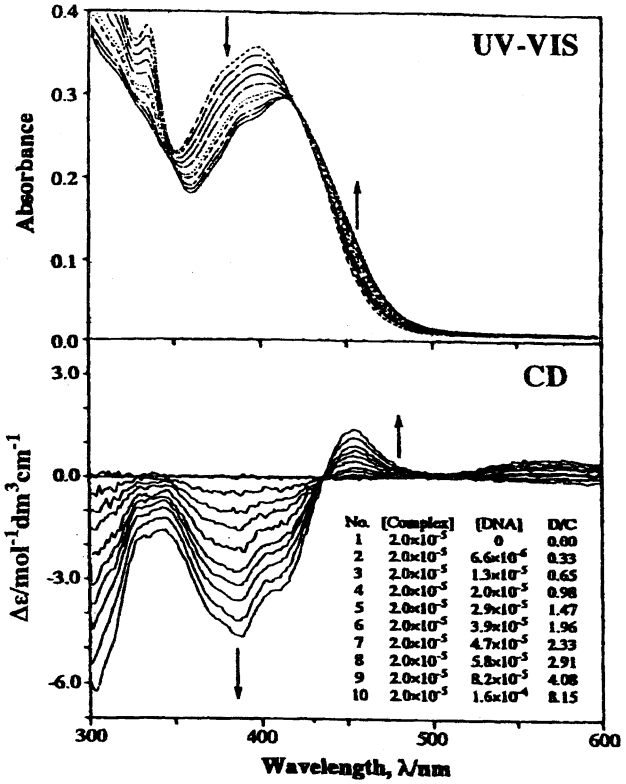

Fig. 5. UV-vis and CD spectral variations of complex **11** by the addition of calf thymus DNA. [Complex]=2.0×10^{-5} M. [DNA]=0—1.6×10^{-4} M. I=0.05 (50 mM NaCl+5 mM HEPES (pH=7.2)). T=25°C. Cell length=1.0 cm (UV-vis). $\Delta\varepsilon$ value is plotted per mol dm^{-3} of complex. The UV-vis and CD spectral variations of complexes **12** and **13** (not drawn) are close to those of **11**.

$$\mathrm{M} + \mathrm{DNA} \rightleftharpoons \mathrm{M\text{-}DNA}, \quad (1)$$

where M-DNA represents the complex-bound DNA. Thus, the binding constants (K_b) for **1**—**9** were analysed based on this equation, as mentioned in the Experimental section.

In the case of **10**—**14**, which have an aromatic *N*,*N*′-bridging group, they exhibited clear UV-vis and CD spectral variations. The typical examples are shown in Figs. 4, 5, and 6. As shown in Figs. 4(A), 5, and 6(A), λ_{max} at near to 400 nm (ε=16900—17900) shifted to near 420 nm (ε=13500—14600) with an isosbestic point at 425 nm by the addition of DNA. In the case of **14**, λ_{max} at 405 nm (ε=18000) shifted to 415 nm (ε=13700) with an isosbestic point at 450 nm. These red shifts and large hypochromic shifts (18—24%) of the charge-transfer bands are clear evidence for intercalation to the base pairs of DNA.[26] In addition, as shown in Figs. 4(B) and 6(B), **10** and **14** exhibit another spectral variation at over R=3.0 (**10**) and 1.3 (**14**). That is, λ_{max} at 420 nm (ε=14600) of **10** shifted to 423 nm (ε=14800) with an isosbestic point at 420 nm with an accompanying hypochromic shift of the shoulder (390 nm) from ε=13700 to ε=12300. In the case of **14**, λ_{max} at 415 nm (ε=13700) shifted to 420 nm (ε=11500) with an isosbestic point at 467 nm. These facts indicate that two kinds of intercalations occur step by step for **10** and **14**. In fact, the induced CD's of **10** and **14** consist of two kinds of CD variations (Figs. 4 and 6), while the induced CD's of **11**—**13** comprise one kind of CD variation, and are very similar to each other (Fig. 5). Since the induced CD's at R=10.7 (**10**) and R=8.3 (**14**) are close to those of **11**—**13** at R=8.2, it becomes clear that the second induced CD's of **10** (over R=3.0) and of **14** (over R=1.3) correspond to the formation of M-DNA species. Further, the presence of an

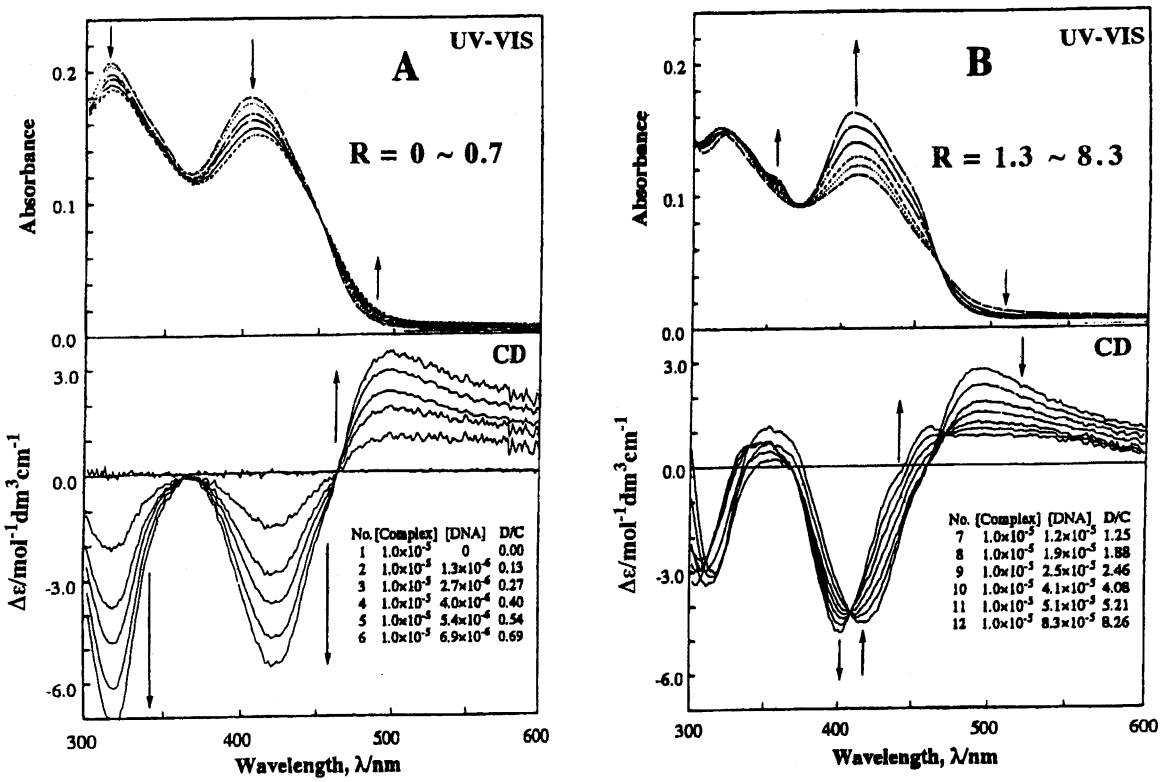

Fig. 6. UV-vis and CD spectral variations of complex **14** by the addition of calf thymus DNA. **A**: R=0—0.7, [Complex]=1.0×10^{-5} M, [DNA]=0—6.9×10^{-6} M. **B**: R=1.3—8.3, [Complex]=1.0×10^{-5} M, [DNA]=1.2—8.3×10^{-5} M. I=0.05 (50 mM NaCl+5 mM HEPES (pH=7.2)). T=25°C. Cell length=1.0 cm (UV-vis). $\Delta\varepsilon$ value is plotted per mol dm^{-3} of complex.

iso-CD point(s), which fall across the CD-base line in the case of **11**—**13**, indicates that the CD variations of **11**—**13** correspond to reaction 1), and that the stepwise CD variations of **10** and **14** correspond to the following reactions:

$$2M + DNA \rightleftarrows M_2\text{-DNA} \quad (\text{at low } R) \tag{2}$$

$$M_2\text{-DNA} + DNA \rightleftarrows 2M\text{-DNA} \quad (\text{at high } R). \tag{3}$$

All of the DNA solutions containing **10**—**14** showed CD with opposite signs at near 260 nm. Hence, it is clear that both the M-DNA and M_2-DNA species keep the B-form double-helix structure.

In the case of **10**—**14**, since they have a structurelly rigid phenylene or naphthylene group as the *N*,*N*′-bridging group, the complexes have difficulty to take a tetrahedrally distorted configuration. Therefore, the intence induced CD at the CT band region of these complexes should mainly come from the effect of asymmetric electronic and magnetic fields of chiral DNA on highly oriented complexes.[24] This high orientation is possible only when the complexes are intercalated into the base pairs of DNA. Indeed, we have observed that about 75% of **10** is oriented to take a dihedral angle of 0°±10° between the coordination plane of **10** and the DNA helix axis in the solid state.[10]

The above UV-vis and CD spectral behaviors strongly support that complexes having an aliphatic *N*,*N*′-bridging group bind to the groove of DNA, whereas those having an aromatic *N*,*N*′-bridging group intercalate to the base pairs of DNA.

Binding Constants with Calf Thymus DNA. The binding constants (K_b) with calf thymus DNA were investigated by applying three experimental methods (equilibrium dialysis, UV-vis, and CD titrations) and two analyzing methods (macroscopic analysis (method I) as well as a microscopic Scatchard plot (method II)). The analytical procedures are described in the Experimental section. All of the plots for methods I gave a straight line (the correlation coefficient=97—99%) through the origin, and the K_b values were estimated from the slope. Also, all of the plots for method II gave a straight line (the correlation coefficient=97—99%) with a minus slop; the K_b and n values were calculated from these slope and intercept. All of the K_b values are summarized in Table 8, together with the n values. The K_b values from three experimental methods are comparable to each other, indicating that the data are highly reliable. Of the three methods, since the CD titration was widly applicable, the K_b values from the CD titration are mainly used in the following discussion.

The K_b values from method I of **1**—**9** are in the range of 0.23—3.5×10^3 M^{-1}, while those of **10**—**14** are in the range of 1.8—38×10^4 M^{-1}, reflecting the difference in the binding modes between the former complexes (groove binding) and the latter ones (intercalation). A similar difference was observed for the K_b values from method II of **1**,**8**,**9**—**13**. The K_b values from method II of **1**,**8**,**9** are close to that of $[Ru(phen)_3]^{2+}$, which is reported to be a groove

Table 8. Binding Constants (K_b) with Calf Thymus DNA of Cationic Schiff Base Complexes of Copper(II)[a)]

Complex	Macroscopic K_b (Method I)/10^3 M^{-1} [b)]			Microscopic K_b (Method II)/10^4 M^{-1} [f)]		
	Equil. Dialysis	UV-vis Titration	CD Titration	Equil. Dialysis	UV-vis Titration	CD Titration
1	1.2	c)	1.0	1.4(7.2)	c)	c)
2	0.52	c)	0.53	c)	c)	c)
3	0.42	c)	0.46	c)	c)	c)
4	0.16	c)	0.36	c)	c)	c)
5	2.5	c)	3.5	c)	c)	c)
6	0.22	c)	0.23	c)	c)	c)
7	0.53	c)	0.43	c)	c)	c)
8	1.3	c)	1.1	c)	c)	1.5(7.4)
9	0.94	c)	0.85	c)	c)	1.3(7.3)
10	d)	52	53	d)	c)	93(7.4)
	d)	42[e)]	41[e)]	d)	31[e)](3.8)	54[e)](4.0)
11	45	34	32	58(2.7)	63(3.2)	71(2.8)
12	32	21	19	25(2.8)	30(3.2)	30(3.0)
13	29	21	18	21(3.0)	25(3.3)	20(2.9)
14	d)	320	375	d)	d)	d)
	d)	94[e)]	100[e)]	d)	d)	d)

a) HEPES=5.0 mM (pH=7.2), NaCl=50 mM, 25 °C. b) K_b=[M-DNA]/[M][DNA]. c) The variation of UV-vis or CD spectra was too small to estimate K_b. d) Formation of PPT. e) K_{b2} (K_{b2}=[M_2-DNA]/[M][M-DNA]). f) Site size pairs (n) in parenthesis.

binder.[27,28)] The K_b values of **10**—**14** correspond to those of $[Ru(phen)_2(phi)]^{2+}$ and $[Ru(bpy)_2(phi)]^{2+}$, which are known to be a strong intercalator.[27)] In the case of **10** and **14**, the K_{b2} value is close to the K_{b1} value, supporting the idea that the process for K_{b2} also corresponds to the intercalation. Since the binding constants of **14** (bridge=naphthylene) are about 10-times or much higher than those of **10**—**13** (bridge=phenylene), it is suggected that the intercalation occurs with the aromatic bridging groups.

The K_b values decrease in the order **1** >**2** >**3** >**4**, and in the order **10** >**11** >**12** >**13**. Since the orders correspond to the increasing order of the steric bulkiness of the NR_3 group, it is clear that the NR_3 causes a steric hindrance rather than hydrophobic binding. On the other hand, the K_b of **5**, which has *t*-buthyl groups at the 3,3′-positions of the Schiff base ligand, is 3.5-times higher than that of 1, suggesting that a hydrophobic interaction is concerned in the groove binding of **5**, in addition to the electrostatic interaction. The substituent effect of an *N*,*N*′-ethylene bridge is complicated. The K_b values decrease in the order **1** >**6** >**7**, which suggests that the methyl and methylene substituents at the *N*,*N*′-ethylene bridge bring about a steric hindrance. In contrast to this, in the case of **8** and **9**, which have a cyclohexylene substituent, the K_b values are close to that of **1**, and the K_b of **8** (*R*,*R*-isomer) is 1.3-times higher than the K_b of **9** (*S*,*S*-isomer), thus suggesting that the configuration of the *N*,*N*′-bridging group also affects on the groove binding of these complexes.

Site Size Base Pairs. The data are listed in Table 8. The value of the site size base pairs (n) for **1**,**8**, and **9** is about 7.3, which corresponds to that the minimal averaged interval of DNA base pairs between the neighboring complexes bound on the DNA is 7.3 (the pitch length=24.8 Å). On the other hand, the molecular size of the long axis of **1** (intramolecular distance between two cationic nitrogen atoms (16.4 Å)+2 (van der waals radii of $[N(CH_3)_4]^+$)) is calculated to be ca. 20 Å on the basis of the X-ray crystal data of **1**. The molecular size of the complexes and DNA is illustrated in Fig. 7. Since the molecular size of **1** is at least shorter than the pitch length (24.8 Å), the n value seems to be reasonable as the groove binding of **1**. Since the molecular size of the long axis of **8** and **9** is close to that of **1**, it is also reasonable that **1**,**8**, and **9** exhibit a nearlly equal n value. It is known that the n value of the groove binder, $[Ru(bpy)_3]^{2+}$, is 6—12, and that this value is larger than n=4 of the intercalator, $[Ru(bpy)_2(phi)]^{2+}$.[27)]

Quite similar to the ruthenium complexes, the n value of **10**—**13** is 3—4, and is clearly smaller than that of **1**,**8**, and **9**. Although the n value for K_{b1} of **10** is 7.4, this value corresponds to the first step of the two steps of the reaction, and dose not correspond to the n value for fully occupied DNA by **10**. The smaller n value (3—4) corresponds to the pitch length of 10.2—13.6 Å, and is reasonable as the intercalation. Because, the molecular size of the long axis of **10**—**13**

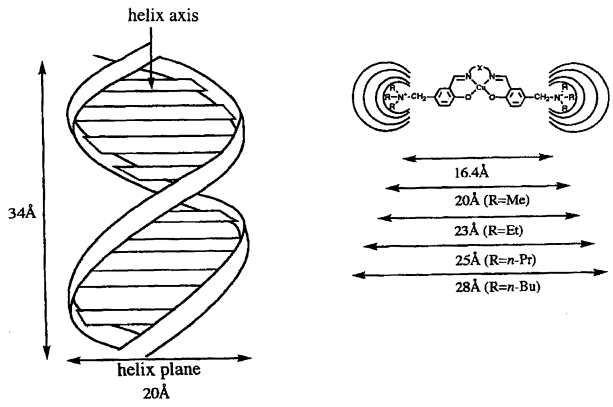

Fig. 7. Relation of the sizes of B-form DNA and cationic Schiff-base complexes.

is estimated to be about 20, 23, 25, and 28 Å, respectively (Fig. 7), it is quite difficult that a molecule with long size of more than 20 Å can be oriented within a DNA pitch length of 10.2—13.6 Å by any other way than intercalation. Since the molecular size (20 Å) of **10** is close to the size of the DNA helix plane (20 Å), **10** has a sterically well fitted size to intercalate to B-form DNA with its phenylene group. On the other hand, in spite of the longer molecular size (23—28 Å) of **11**—**13**, they have a similar n value to that of **10**. This may be due to the fact that the R part of the NR_3 group is oriented outside of the DNA helix plane when the complexes intercalate to the base pairs with the phenylene group.

Salt Dependency of K_b Values. It has recently been reported that the salt dependency of the binding constants of cationic complexes with DNA is an effective method to discriminate the difference between the intercalation and groove binding.[28] This method is based on the fact that the cationic grove binder recieves the effect of ionic strength more strongly than dose the cationic intercalater having the same charge as the groove binder. This is because the contribution of the electrostatic interaction between the cationic complex and anionic DNA on the total binding energy is relatively higher in groove binding than in intercalation. We thus investigated the salt dependency of the K_b values of typical complexes (**1**,**4**,**10**, and **13**) to confirm the difference in the binding mode between **1**,**4** (groove binding) and **10**,**13** (intercalation).

As shown in Fig. 8, the slope of the plots of $\log K_b$ vs. $\log [Na^+]$ is -1.0 for both K_{b1} and K_{b2} of **10**, and is -1.2 for **13**; the values are obviously smaller in the minus direction than the slope for **1** (-1.7) and **4** (-1.8). Accordingly, this fact well supports our result that **1** and **4** act as a groove binder, whereas **10** and **13** as intercalater. In addition, the close value of the slope between K_{b1} and K_{b2} for **10** supports the idea that the both processes correspond to the intercalation.

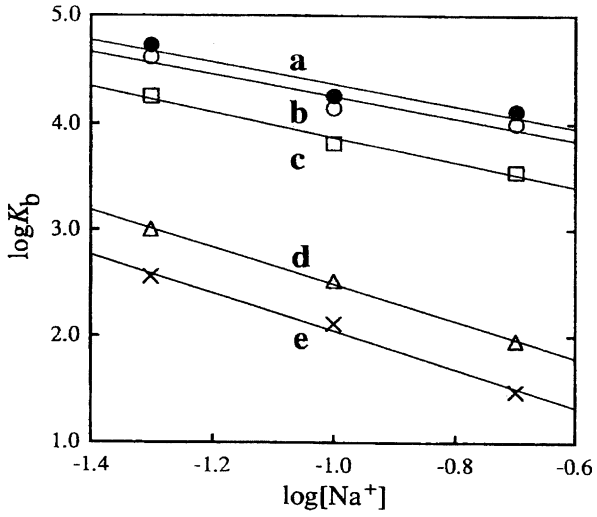

Fig. 8. Salt dependence of binding constants (K_b). **a**: complex **10** (K_{b1}). **b**: complex **10** (K_{b2}). **c**: complex **13**. **d**: complex **1**. **e**: complex **4**.

Interactions with Poly(dA-dT)–poly(dA-dT), Poly(dG-dC)–poly(dG-dC), and Poly(dA-dC)–poly(dT-dG). The induced CD spectra behaviors of selected complexes **1** and **10** in the presence of AT-DNA, GC-DNA, and ACTG-DNA are shown in Figs. 9 and 10. The B-form structure of the artificial DNA's was confirmed from the CD spectra at near to 260 nm. The binding constants (method I) with these DNA's are listed in Table 9.

In the case of **1**, the binding constants increase in the order GC-DNA=ACTG-DNA < AT-DNA, indicating that **1** has the affinity for AT-DNA. Further, the induced CD by calf thymus DNA is very similar to that by AT-DNA, but not to

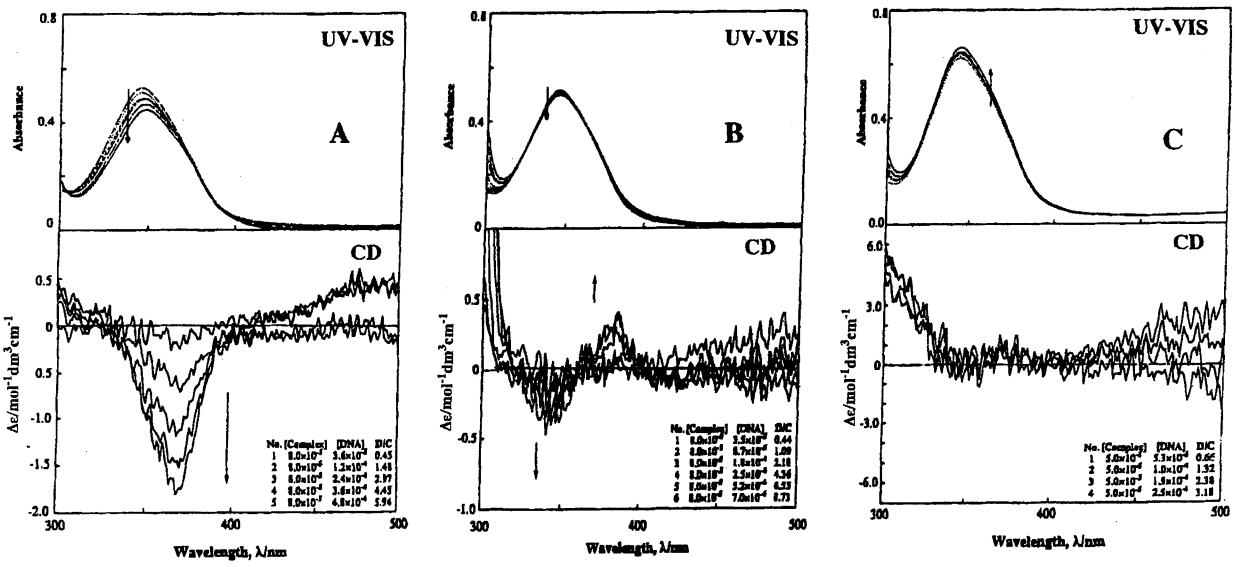

Fig. 9. UV-vis and CD spectral variations of complex **1**. **A**: poly(dA-dT)–poly(dA-dT). **B**: poly(dG-dC)–poly(dG-dC). **C**: poly(dA-dC)–poly(dT-dG). [Complex]=8.0×10^{-5} M for **A** and **B**, and 5.0×10^{-5} M for **C**. [DNA]=0—4.8×10^{-4} M for **A**, 0—7.0×10^{-4} M for **B**, and 0—2.5×10^{-4} M for **C**. I=0.05 (50 mM NaCl+5 mM HEPES (pH=7.2)). T=25°C. Cell length=1.0 cm for UV-vis spectra. $\Delta\varepsilon$ value is plotted per mol dm^{-3} of complex.

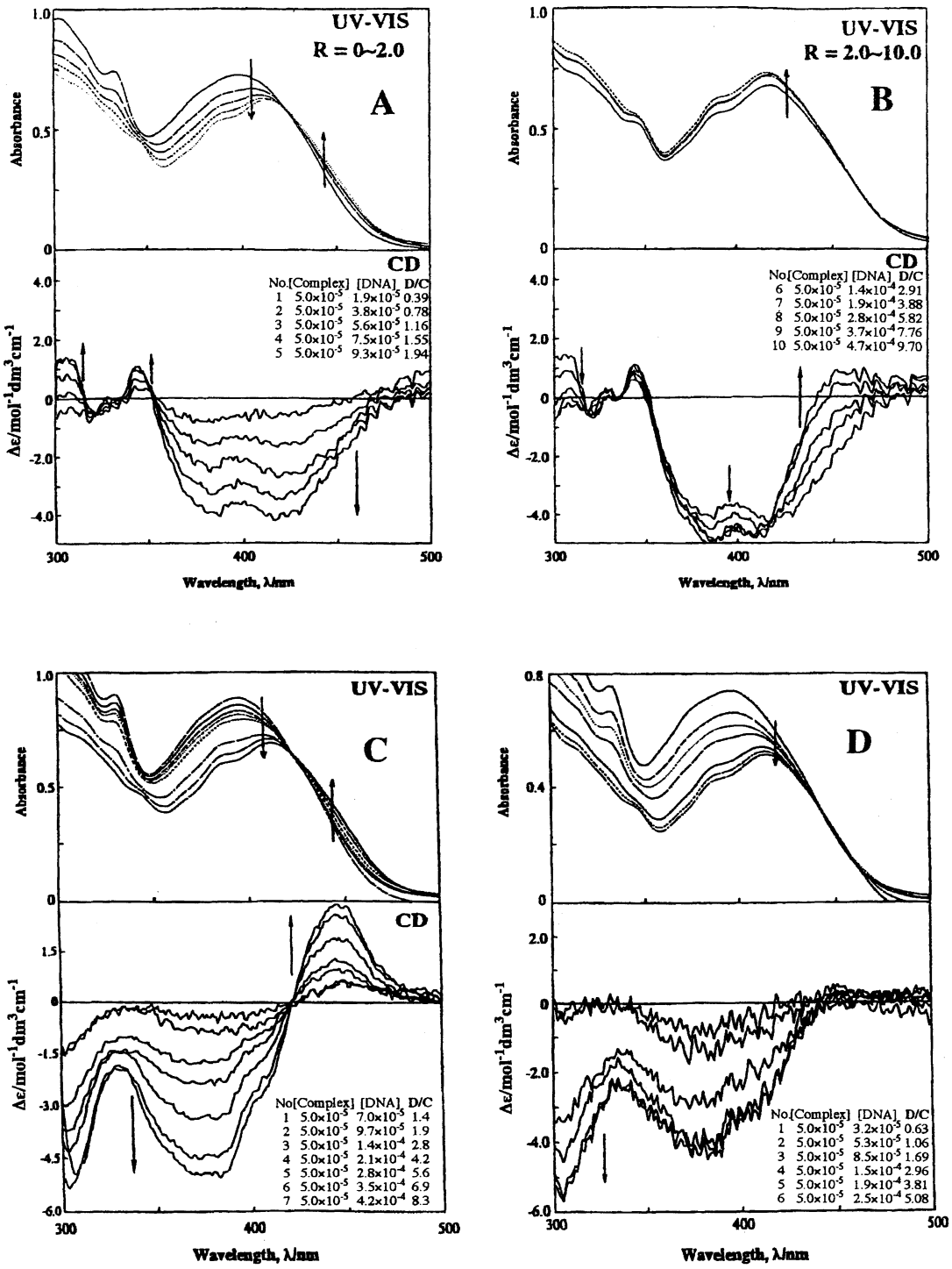

Fig. 10. UV-vis and CD spectral variations of complex **10**. **A**: poly(dA-dT)–poly(dA-dT) at low *R*. **B**: poly(dA-dT)–poly(dA-dT) at high *R*. **C**: poly(dG-dC)–poly(dG-dC). **D**: poly(dA-dC)–poly(dT-dG). [Complex]=5.0×10^{-5} M. [DNA]=0—9.7×10^{-5} M for **A**, 1.5—4.8×10^{-4} M for **B**, 0—3.1×10^{-4} M for **C**, and 0—2.5×10^{-4} M for **D**. I=0.05 (50 mM NaCl+5 mM HEPES (pH=7.2)). T=25°C. Cell length=1.0 cm for UV-vis spectra. $\Delta\varepsilon$ value is plotted per mol dm^{-3} of complex.

those by GC-DNA and ACTG-DNA, indicating that complex **1** is fond of an AT-rich region of calf thymus DNA; this result is consistent with the fact that Mn(III)-salen exhibits AT-site selectivity.[9a)]

In the case of **10**, the binding constants increase in the order GC-DNA < ACTG-DNA < AT-DNA, indicating that **10** also has affinity for AT-DNA. In addition, the K_{b1} and K_{b2} values for AT-DNA are comparable to those for calf thymus DNA, suggesting the affinity for the AT-rich region of calf thymus DNA. The induced CD by AT-DNA comprises two kinds of CD variation, which is consistent with the behavior for calf thymus DNA. However, the induced CD's by GC-

Table 9. Binding Constants (K_b) with Poly(dA-dT)–poly-(dA-dT), Poly(dG-dC)–poly(dG-dC), and Poly(dA-dC)–poly(dT-dG)

Complex	Macroscopic K_b (Mehtod I) /$10^3 M^{-1}$ a)		
	Poly(dA-dT) –poly(dA-dT)	Poly(dG-dC) –poly(dG-dC)	Poly(dA-dC) –poly(dT-dG)
1	3.8	1.0	ca. 1.0
10	47(33)b)	8.3	9.9

a) Data from CD titration, HEPES=5 mM (pH=7.2), NaCl=50 mM, 25 °C. b) K_{b2} value in parenthesis.

DNA and ACTG-DNA each comprise only one CD variation, and the behavior is different from that for calf thymus DNA. Therefore, on the basis of these facts, it can be concluded that complex **10** exhibits an affinity for the AT-base pairs of calf thymus DNA, although the induced CD spectra by AT-DNA are somewhat different from those by calf thymus DNA. This difference may be because calf thymus DNA comprises various kinds of AT-rich regions, and because the AT-base pairs selectivity of **10** is not necessarily very high, as expected from the K_b values in Table 9.

Conclusion

A series of cationic Schiff base complexes of copper(II), **1**—**14**, was newly prepared, and the planar N_2O_2 coordination structure was confirmed from an X-ray crystal structure analysis of **1** and the UV-vis and ESR spectra of the complexes. From the appearant stability constants at pH=7.2 and the dimer formation constants of **1**,**10**,**12** and **14**, the following facts were confirmed: 1) The complexes have substantial stability for ligand substitution and 2) The complexes exist as monomers at low concentrations (10^{-4}—10^{-5} M).

Complexes **1**—**9**, which have an aliphatic *N*,*N*′-bridging group, selectively bind to the groove of DNA by electrostatic and hydrophobic interactions. This was confirmed from the small UV-vis spectral variation at the CT-band region by the addition of DNA, the appearance of an induced CD spectra at the CT-band region by the addition of DNA, the comparatively low binding constants (K_b) with calf thymus DNA, and the relatively high salt dependence of K_b. In addition, it became clear from the K_b's and the induced CD spectra in the presence of AT-DNA, GC-DNA, and ACTG-DNA that **1** shows AT-sequence selectivity.

Complexes **10**—**14**, which have an aromatic *N*,*N*′-bridging group, selectively intercalated to the base pairs of DNA. This was confirmed from the red shift and hypochromic shift of the UV-vis spectra at the CT-band region upon the addition of DNA, the appearance of induced CD spectra at the CT-bands upon the addition of DNA, the high binding constants (K_b) with calf thymus DNA, and the relatively low sensitivity for the salt dependence of K_b. In addition, it was found that **10** and **14** intercalate to the base pairs of DNA in two steps of equilibrium, and that **10** exhibits AT-base pairs selectivity.

A part of this work was supported by a Grant-in-Aid for Scientific Research No. 0764735 from the Ministry of Education, Science and Culture.

References

1) a) T. D. Tullius, "Metal–DNA Chemistry," ACS Symposium Series 402, American Chemical Society, Washington, D.C. (1989); b) I. Bertini, H. B. Gray, S. J. Lippard, and J. S. Valentine, "Bioinorganic Chemistry," University Science Books, Mill Valley (1994); c) Chemical Society of Japan, "New Development of Bio-Inorganic Chemistry," Gakkai Syuppan Center, Tokyo (1995), No. 24; d) Chemical Society of Japan, "Biological Activity of Trace Metals," Gakkai Syuppan Center, Tokyo (1995), No. 27.

2) a) J. Reedijk, *Pure Appl. Chem.*, **59**, 181 (1987); b) L. A. Basile and J. K. Barton, *Met. Ions. Biol. Syst*, **25**, 31 (1989); c) A. M. Pyle and J. K. Barton, *Prog. Inory. Chem.* , **38**, 413 (1990); d) B. Lippert, *Prog. Inorg. Chem.*, **38**, 1 (1990); e) D. S. Sigman, A. Mazumder, and D. M. Perrin, *Chem. Rev.*, **93**, 2295 (1993); g) G. Prativiel and J. Meunier, *Angew. Chem., Int. Ed. Engl.*, **34**, 746 (1995); h) P. M. Takahara, A. C. Rosenzweig, C. A. Frederick, and S. J. Lippard, *Nature*, **337**, 649 (1995); i) M. Otsuka, M. Fujita, T. Aoki, S. Ishii, Y. Sugiura, T. Yamamoto, and J. Inoue, *J. Med. Chem.*, **38**, 3264 (1995).

3) Recent articles: a) S. C. K. Elmroth and S. J. Lippard, *Inorg. Chem.*, **34**, 5234 (1995); b) C. S. Peyratout, T. K. Aldridge, D. K. Crites, and D. R. McMillin, *Inorg. Chem.*, **34**, 4484 (1995); c) W. A. Kalsbeck and H. H. Thorp, *J. Am. Chem. Soc.*, **115**, 7146 (1993).

4) Recent articles: a) C. Turro, S. H. Bossmann, Y. Jenkins, J. K. Barton, and N. J. Turro, *J. Am. Chem. Soc.*, **117**, 9026 (1995); b) N. Grover, T. W. Welch, T. A. Fairley, M. Cory, and H. H. Thorp, *Inorg. Chem.*, **33**, 3544 (1994); c) N. Y. Sardesai, K. Zimmermann, and J. K. Barton, *J. Am. Chem. Soc.*, **116**, 7502 (1994).

5) F. Liu, K. A. Meadows, and D. R. McMillin, *J. Am. Chem. Soc.*, **115**, 6699 (1993).

6) N. Colocci, M. D. Distefano, and P. B. Dervan, *J. Am. Chem. Soc.*, **115**, 4468 (1993).

7) G. Pratviel, V. Duarte, J. Bernadou, and B. Meunier, *J. Am. Chem. Soc.*, **115**, 7939 (1993).

8) M. Shionoya, T. Ikeda, E. Kimura, and M. Shiro, *J. Am. Chem. Soc.*, **116**, 3848 (1994).

9) a) D. J. Gravert and J. H. Griffin, *Inorg. Chem.*, **35**, 4837 (1996); b) D. J. Gravert and J. H. Griffin, *J. Org. Chem.*, **58**, 820 (1993); c) S. A. Woodson, J. G. Muller, C. J. Burrows, and S. E. Rokita, *Nucleic Acids Res.*, **21**, 5524 (1993); d) C. J. Burrows and S. E. Rokita, *Acc. Chem. Res.*, **27**, 295 (1994); e) S. Bhattacharya and S. S. Mandal, *J. Chem. Soc., Chem. Commun.*, **1995**, 2489; f) S. Routier, J-L. Bernier, M. J. Warninig, P. Colson, C. Houssier, and C. Bailly, *J. Org. Chem.*, **61**, 2326 (1996).

10) K. Sato, M. Chikira, Y. Fujii, and A. Komatsu, *J. Chem. Soc., Chem. Commun.*, **1994**, 625.

11) S. J. Angyal, P. J. Morris, J. R. Tetaz, and J. G. Wilson, *J. Chem. Soc.*, **1950**, 2141.

12) Y. Ogata, A. Kawasaki, and F. Sugiura, *Tetrahedron*, **24**, 5001 (1968).

13) R. G. Asperger and C. F. Liu, *Inog. Chem.*, **4**, 1492 (1965). For the absolute configuration: F. Marumo, Y. Utsumi, and Y. Saito, *Acta Crystallogr., Sect. B*, **26**, 1492 (1970).

14) R. Sayre, *J. Am. Chem. Soc.*, **77**, 6689 (1955).

15) a) J. Stary, *Anal. Chim. Acta*, **28**, 132 (1963); b) G. Anderegg, *Helv. Chim. Acta*, **47**, 1801 (1964).

16) L. G. Marzilli, P. A. Marzilli, and J. Helpern, *J. Am. Chem. Soc.*, **93**, 1374 (1971).

17) C. R. Cantor and R. R. Schimmel, "Biophysical Chemistry," W. H. Freeman and Company, San Francisco (1980), Part III, Chap. 15.
18) S. J. Gruber, C. M. Harris, and E. Sinn, *J. Inorg. Nucl. Chem.*, **30**, 1805 (1968).
19) R. S. Downing and F. L. Urbach, *J. Am. Chem. Soc.*, **91**, 5977 (1969).
20) a) D. Hall and T. N. Waters, *J. Chem. Soc.*, **1960**, 2644; b) E. N. Baker, D. Hall, and T. N. Waters, *J. Chem. Soc. A*, **1970**, 400; c) E. N. Baker, D. Hall, and T. N. Waters, *J. Chem. Soc. A*, **1970**, 406.
21) E. Sinn and C. M. Harris, *Coord. Chem. Rev.*, **4**, 391 (1969).
22) A. D. Toy, M. D. Hobday, P. D. W. Boyd, and T. D. Smith, *J. Chem. Soc., Dalton Trans.*, **1973**, 1259.
23) M. Chikira, H. Yokoi, and T. Isobe, *Bull. Chem. Soc. Jpn.*, **47**, 2208 (1974).
24) a) R. Lyng, T. Hard, and B. Norden, *Biopolymers*, **26**, 1327 (1987); b) R. Lyng, A. Rodger, and B. Norden, *Biopolymers*, **31**, 1709 (1991); c) R. Lyng, A. Rodger, and B. Norden, *Biopolymers*, **32**, 1201 (1992).
25) W. Zaenger, "Principles of Nucleic Acid Structure," Springer-Verlag, New York (1984).
26) E. C. Long and J. K. Barton, *Acc. Chem. Res.*, **23**, 271 (1990).
27) A. M. Pyle, J. P. Rehamann, R. Meshoyrer, C. V. Kumar, N. J. Turro, and J. K. Barton, *J. Am. Chem. Soc.*, **111**, 3051 (1989).
28) S. Satyanarayana, J. C. Dabrowiak, and J. B. Chaires, *Biochemistry*, **31**, 9319 (1992).